Supplementary Information

Table of contents

Supplementary Note 1. Additional validation of NQC-PACE across diverse Fe–H environments

Supplementary Fig. 1 shows the relative stability of hydrogen in strained bulk α-Fe. PACE, NQC-PACE, DFT and DFT+ZPE were compared for a tetrahedral (T) site under isotropic strain and for tetrahedral and octahedral (O) sites under uniaxial strain. Except for H_2 in Supplementary Fig. 2, hydrogen binding energies are defined relative to hydrogen dissolved at a T site in unstrained bulk α-Fe. PACE reproduces the strain dependence obtained from DFT, whereas the effect of nuclear quantum corrections predicted by NQC-PACE is consistent with the trend obtained from DFT+ZPE. In particular, pronounced quantum stabilisation is observed for the O-site environment.

Supplementary Fig. 2 provides additional validation for representative Fe–H environments not shown individually in Fig. 2. For an edge dislocation, a Σ5(310) symmetric tilt grain boundary and low-index surfaces, PACE reproduces the site-dependent hydrogen stability obtained from DFT. For the edge-dislocation sites, the DFT and DFT+ZPE values were taken from a previous first-principles study[1]. The nuclear quantum corrections predicted by NQC-PACE also follow the trends obtained from DFT+ZPE across these different local environments. NQC-PACE further provides a consistent description of the bond-length dependence of the H_2 binding energy.

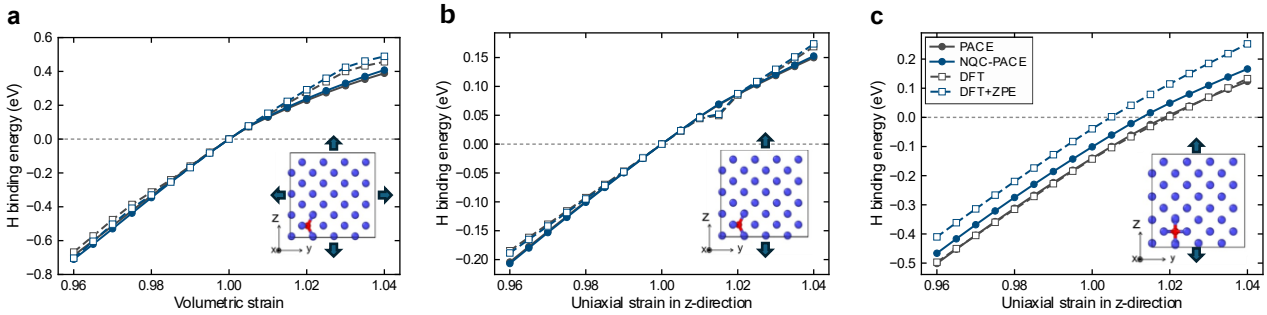

Supplementary Fig. 1 | Validation of hydrogen stability in strained bulk α-Fe.

a, H binding energy at a tetrahedral (T) site in α-Fe under isotropic strain. **b**, H binding energy at a T site under uniaxial strain applied along the z direction. **c**, H binding energy at an octahedral (O) site under the same uniaxial strain. Results obtained with PACE, NQC-PACE, DFT and DFT+ZPE are compared. All energies are referenced to hydrogen dissolved at a T site in unstrained bulk α-Fe, with positive values indicating stabilisation relative to this reference state. Insets schematically illustrate the applied strain and the H site.

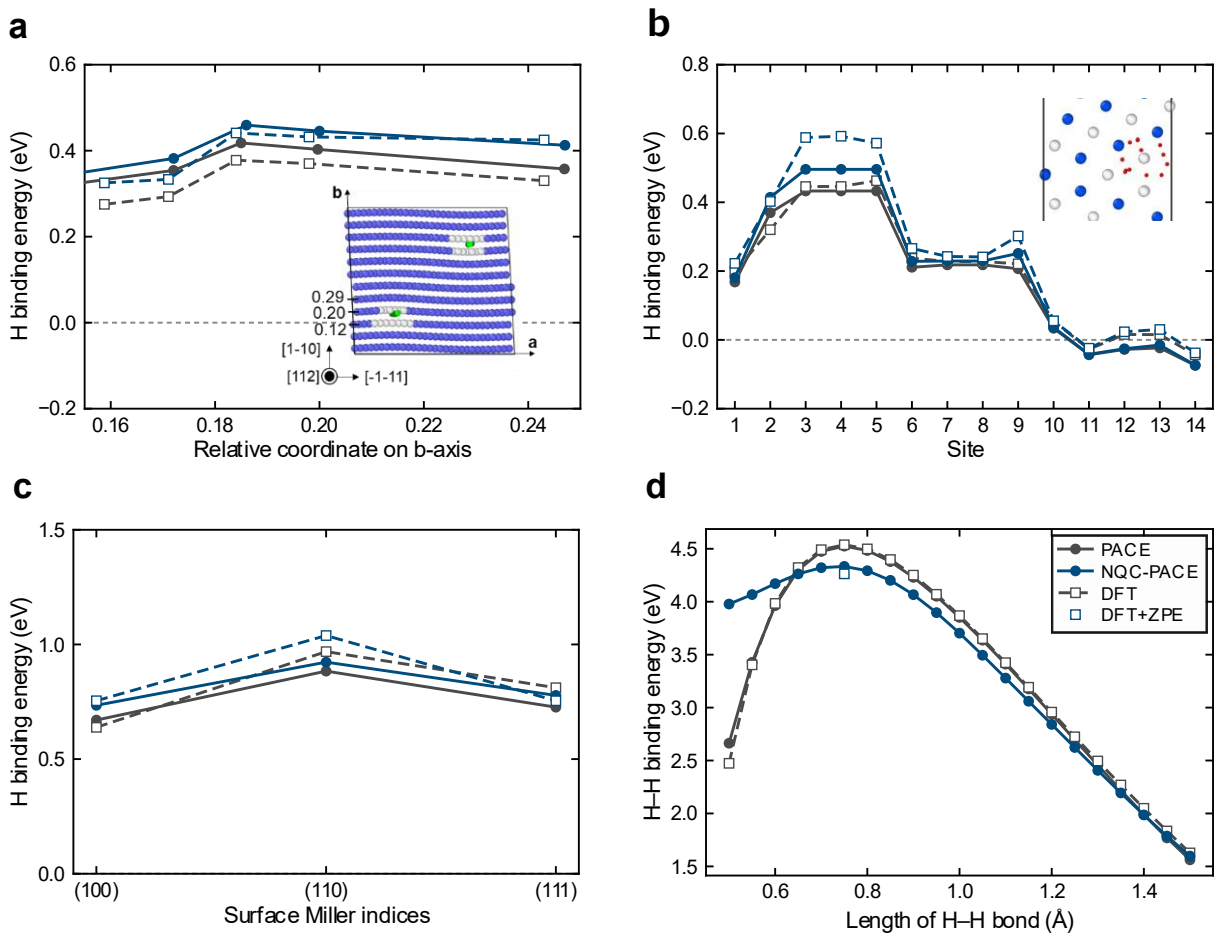

Supplementary Fig. 2 | Additional validation for representative lattice defects, surfaces and H_2. **a**, H binding energies at sites near an edge dislocation in α-Fe, plotted as a function of the relative coordinate along the b axis. The DFT and DFT+ZPE values were taken from a previous first-principles study[1]. **b**, H binding energies at representative sites of a Σ5(310) symmetric tilt grain boundary. **c**, H binding energies at the most stable sites of the low-index (100), (110) and (111) surfaces of α-Fe. For **a–c**, energies are referenced to hydrogen dissolved at a T site in unstrained bulk α-Fe, with positive values indicating stabilisation relative to this reference state. **d**, H–H binding energy as a function of H–H bond length for an isolated H_2 molecule. PACE, NQC-PACE, DFT and DFT+ZPE results are compared where applicable. Insets show representative atomic structures.

Supplementary Note 2. Convergence of PIMD conditions for NQC-PACE force labeling

To determine the computational conditions for the quantum mean-force labels used to train NQC-PACE, we evaluated the convergence with respect to the number of ring-polymer beads, equilibration length, production length, and time step. For each parameter, the quantum force correction, defined as the difference between the mean force obtained from PIMD and the force predicted by the parent PACE potential, was compared with that obtained using a stricter reference condition.

Supplementary Fig. S3 compares the quantum force corrections obtained using the adopted and reference conditions. The quantum force corrections obtained using 32 beads, 6000 equilibration steps, 10000 production steps, and a time step of 1.0 fs show good agreement with those obtained using the corresponding reference conditions of 48 beads, 10000 equilibration steps, 20000 production steps, and a time step of 0.5 fs, respectively. The RMSE over all force components ranges from 0.67 to 1.12 meV $Å^{-1}$, which is sufficiently small compared with the range of the quantum force corrections, extending to approximately 1 eV $Å^{-1}$. Good agreement with the reference values is also obtained for the force components of both Fe and H atoms, with no clear systematic deviation even in regions exhibiting large quantum force corrections. These results indicate that the quantum mean forces required for NQC-PACE training are sufficiently converged under the adopted conditions. Accordingly, 32 beads, 6000 equilibration steps, 10000 production steps, and a time step of 1.0 fs were used for PIMD force labeling in this study.

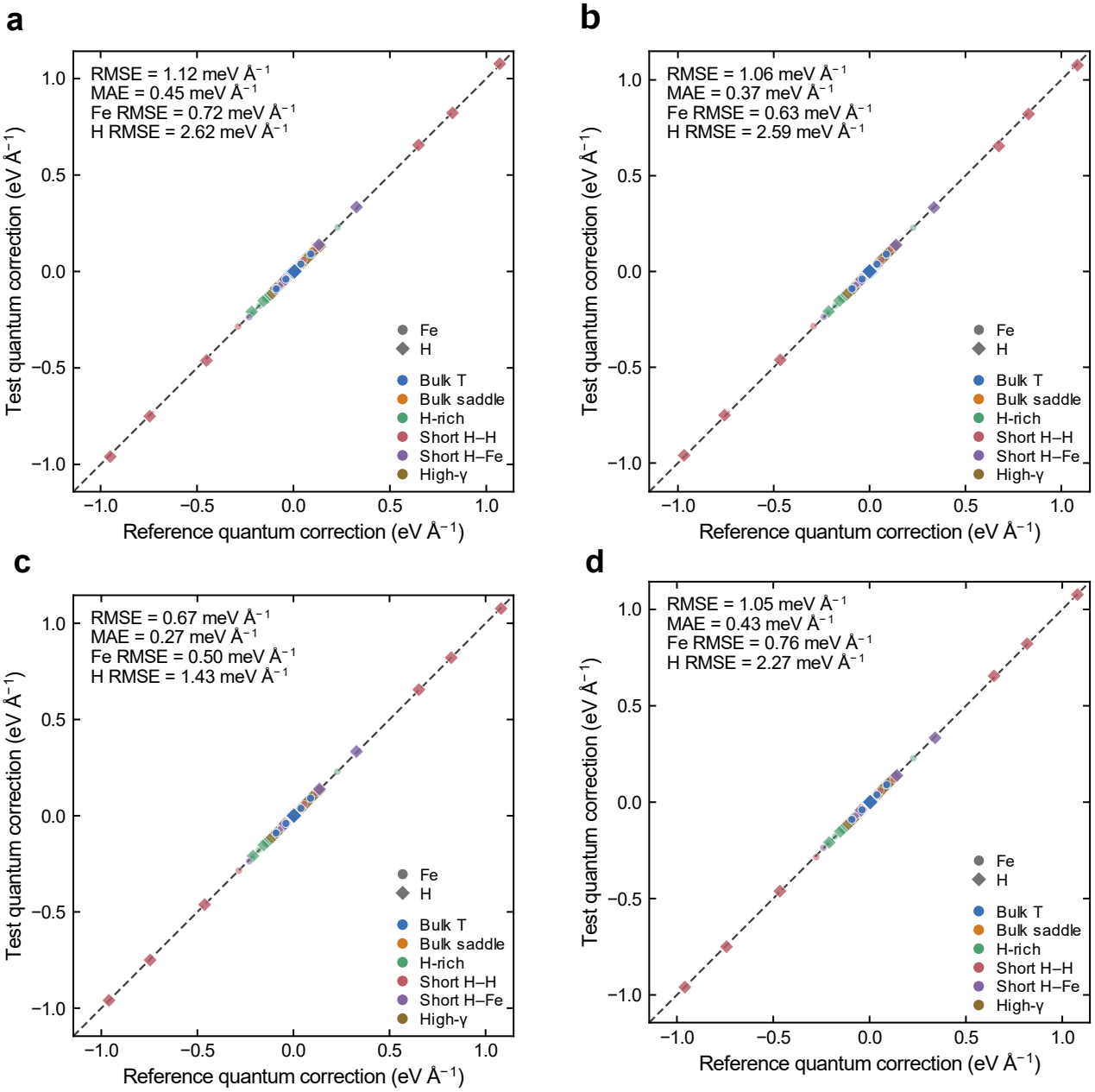

Supplementary Fig. 3 | Convergence of the PIMD conditions for NQC-PACE force labeling. Comparison of the quantum force corrections obtained using the adopted PIMD conditions with those obtained using stricter reference conditions: (a) 32 versus 48 beads, (b) 6000 versus 10000 equilibration steps, (c) 10000 versus 20000 production steps, and (d) time steps of 1.0 versus 0.5 fs. The quantum force correction is defined as the difference between the PIMD mean force and the force predicted by the parent PACE potential. Each point represents a Cartesian force component of an individual atom; colors indicate representative Fe–H atomic environments, and symbols denote Fe and H atoms. The dashed line indicates perfect agreement. For all tested parameters, the deviations from the reference calculations are sufficiently small compared with the overall range of the quantum force corrections.

Supplementary References

1 Yamaguchi, M., Ebihara, K.-i. & Itakura, M. First-principles calculations of hydrogen trapping energy at an edge dislocation core in iron. *Scr. Mater.* **268**, 116887 (2025). https://doi.org/10.1016/j.scriptamat.2025.116887